

See discussions, stats, and author profiles for this publication at: <https://www.researchgate.net/publication/231651839>

Role of Redox Reaction and Electrostatics in Transition-Metal Impurity-Promoted Photoluminescence Evolution of Water-Soluble ZnSe Nanocrystals

ARTICLE *in* THE JOURNAL OF PHYSICAL CHEMISTRY C · APRIL 2009

Impact Factor: 4.77 · DOI: 10.1021/jp810165p

CITATIONS

39

READS

40

6 AUTHORS, INCLUDING:



Hao Zhang

North Sichuan Medical College

264 PUBLICATIONS 4,595 CITATIONS

[SEE PROFILE](#)



Yue Tang

Monash University (Australia)

20 PUBLICATIONS 487 CITATIONS

[SEE PROFILE](#)



Xi Yao

Institute of Chemistry, Chinese Academy of...

16 PUBLICATIONS 140 CITATIONS

[SEE PROFILE](#)



Yang Bai

Iowa State University

446 PUBLICATIONS 9,331 CITATIONS

[SEE PROFILE](#)

Role of Redox Reaction and Electrostatics in Transition-Metal Impurity-Promoted Photoluminescence Evolution of Water-Soluble ZnSe Nanocrystals

Jishu Han, Hao Zhang,* Yue Tang, Yi Liu, Xi Yao, and Bai Yang

State Key Laboratory of Supramolecular Structure and Materials, College of Chemistry, Jilin University, Changchun 130012, P. R. China

Received: November 19, 2008; Revised Manuscript Received: March 12, 2009

In this article, the experimental variable-dependent photoluminescence (PL) evolution of transition-metal-doped ZnSe nanocrystals (NCs) is analyzed by combining the redox reaction and the electrostatics of aqueous NCs. Bulk doping of NCs involves two steps — surface adsorption of the metal impurities and the followed internal doping. The former relates to the electrostatics of aqueous NCs, whereas the latter relates to a redox reaction between the impurities and mercapto-ligands. Both of them occur on the NC surface. In this context, aqueous NCs are essentially charge-stabilized particles. The electrostatic factors that weaken the electrostatic repulsion will facilitate the adsorption of metal impurities on NC surfaces, thus benefiting the surface redox reaction. It furthermore promotes the internal doping of the metal impurities. Consequently, the trap emission and the PL evolution of NCs are facilitated. Besides, the internal doping is favored for the metal impurities with high reduction potential because they are easily reduced by mercapto-ligands. Furthermore, because the presence of metal impurities in NC solution both promotes the oxidation of mercapto-ligands and weakens the interparticle electrostatic repulsion, the colloidal solution of doped aqueous NCs is theoretically proved unstable.

Introduction

To achieve the practical applications of quantum confinement effect, the colloidal synthesis techniques of semiconductor nanocrystals (NCs) have been well established.^{1–4} Typically, the synthetic protocol of CdSe NCs has been foremost developed through the thermal decomposition of organometallic precursor at high temperature (between 250 and 300 °C).¹ The preformed NCs indicate high photoluminescence quantum yields (PLQYs), narrow size distribution, and especially size- and shape-tunable optical and electric properties.^{1–4} Consequently, NC-based materials are potentially applicable in lighting devices, solar cells, biological labels, and so forth.^{5–9} To date, considerable efforts are continuously devoted to the development of new synthetic methods.

Among the recent advances in NC synthesis, green chemistry concepts are particularly emphasized; namely, synthesizing NCs with environment- and user-friendly solvents and raw materials, low energy consumption, and low waste.^{10–13} In this scenario, therefore, various alternative routes are under investigation. The original organometallic approach for the synthesis of high-quality CdSe NCs has been improved through using relative safe, common, and low-cost compounds as the reaction precursors and organic solvents, making the derivative protocols suitable for synthesizing various II–VI and III–V semiconductor NCs.^{14,15} On the basis of early research, highly luminescent CdTe NCs have been prepared using water as the solvent.^{16–19} The utility of water greatly reduces the waste of organic solvents. Besides, a variety of auxiliary techniques, such as hydrothermal synthesis, microwave-assistant synthesis, sonochemical synthesis, and chemical aerosol flow synthesis, have been applied to promote NC growth.^{20–27} These techniques reduce the energy consumption for maintaining NC growth. Most recently, because

of the intrinsic toxicity of Cd-, Hg-, and Pb-containing NCs, the synthesis of nonheavy metal-containing NCs, such as ZnS and ZnSe, has also been noticed, which is expected to make nanosynthesis closer to green chemistry.^{28–32}

Because of the large band gap energy of ZnSe NCs (2.7 eV), transition-metal Cu or Mn impurities are usually introduced into NCs to modulate their PL emission; namely, the synthesis of Cu- or Mn-doped ZnSe NCs (ZnSe:Cu or ZnSe:Mn).^{31–44} These doped NCs exhibit multicolor emissions, which are quite different from the undoped ones.^{45–49} However, the mechanism of formation process of doped NCs is still not fully understood. It is not clear whether this process is kinetics-favored or thermodynamics-facilitated, and especially how to control the size and PL of the preformed NCs. Peng et al. have investigated the growth mechanism of ZnSe:Cu NCs in organic solution.^{31,32} The formation of doped NCs is found dependent both on the adsorption of Cu impurity on ZnSe core at the nucleation stage and on the growth of ZnSe overcoat at the growth stage. These two stages are mainly determined by the species of capping ligands and the temperature used.³² In comparison to the synthesis of NCs in organic solvents, the growth surroundings of aqueous NCs are more complex,^{50–58} owing to the presence of various ions in solution and the environment-sensitive electrostatic interactions.^{59–61} The introduction of metal impurities will undoubtedly increase the complexity of the reaction mixtures, leading to the poor reproducibility of the PLQYs of the preformed NCs. Most importantly, the chemical stability of aqueous doped NCs is usually poor. The preformed NCs will precipitate within weeks or days of storage even in the dark, leading to a rapid decrease of PLQYs. This phenomenon can not be explained according to the photochemical oxidation mechanism.⁶²

Note that aqueous NCs are essentially stabilized by their surface charges. This property determines the aggregation and growth of aqueous NCs as changing the experimental variables.⁶⁰

* To whom the correspondence should be addressed. Fax: +86 431 85193423. E-mail: hao_zhang@jlu.edu.cn

In our previous studies, a colloid stability model is demonstrated to elucidate the influence of experimental variables on the growth rate and PL of aqueous CdTe NCs, which also provides an efficient mean to design and control NC size and PLQYs.^{60,61} In this work, we study the formation process of transition-metal impurity-doped ZnSe NCs by analyzing the redox and electrostatic properties of aqueous NCs. Systematical investigations reveal that the origin of doping foremost relates to a kinetics-favored adsorption of metal impurities with host NCs, which is mainly determined by the electrostatic environment of the NC solution. Next, a redox reaction between metal impurities and mercapto-ligands occurs on NC surfaces, leading to metal impurity doping. The observed PL evolution and the stability of doped ZnSe NCs were mainly determined by the cooperation of redox and electrostatic factors.

Experimental Section

Materials. Selenium powder (-100 mesh, 99.5+ %) and 3-mercaptopropionic acid (MPA, 99+ %) were purchased from Aldrich. NaBH₄ (96%), Zn(NO₃)₂ (99%), CuCl₂ (99%), MnCl₂ (99%), and NaOH (99%) were commercially available products.

Preparation of Aqueous ZnSe, ZnSe:Cu, and ZnSe:Mn NCs. The synthesis of aqueous ZnSe, ZnSe:Cu, and ZnSe:Mn NCs followed a modified preparation of our previous aqueous synthesis technique.⁶³ Typically, freshly prepared NaHSe solution was injected into N₂-saturated aqueous solutions containing Zn(NO₃)₂, Zn(NO₃)₂ and CuCl₂, or Zn(NO₃)₂ and MnCl₂, and MPA with a specific molar ratio, yielding the precursor solution of ZnSe, ZnSe:Cu, or ZnSe:Mn. Before NaHSe addition, the pH of aforementioned solutions was adjusted to basic range using 1 M NaOH. The resulting precursors were refluxed at 100 °C or stored at room temperature to maintain the size and PL evolution of NCs.

Characterization. UV-vis absorption spectra were obtained using a Shimadzu 3100 UV-vis spectrophotometer. Fluorescence spectroscopy was performed with a Shimadzu RF-5301 PC spectrophotometer. The excitation wavelength was 300 nm. All optical measurements were performed at room temperature under ambient conditions. The PLQYs of NCs were estimated at room temperature using quinine in aqueous 0.5 M H₂SO₄ as PL reference.⁶⁴ Transmission electron microscopy (TEM) was conducted using a JEOL-2010 electron microscope at an acceleration voltage of 200 kV. X-ray powder diffraction (XRD) investigation was carried out using Siemens D5005 diffractometer. X-ray photoelectron spectroscopy (XPS) was investigated by using a VG ESCALAB MKII spectrometer with a Mg K α excitation (1253.6 eV). Binding energy calibration was based on C 1s at 284.6 eV. Inductively coupled plasma (ICP) was carried out with PerkinElmer OPTIMA 3300DV analyzer. Zeta potential measurements were performed using a Zetasizer NanoZS (Malvern Instruments). The measurements were carried out immediately after NC preparation to avoid the oxidation of NCs. Because of the uncertainties of zeta potential measurements, each sample was measured 10 times, and the average data were presented.

Results and Discussion

Characterization of ZnSe and Transition-Metal Impurity-Doped ZnSe NCs. Water-soluble ZnSe, ZnSe:Cu, and ZnSe:Mn NCs were prepared directly in aqueous solutions using MPA as capping ligand.⁶³ The corresponding precursors were refluxed at 100 °C for different intervals to maintain the growth of NCs, which promoted the size and PL evolution. Figure 1 indicated the typical XRD pattern and TEM images of ZnSe:Cu and ZnSe:

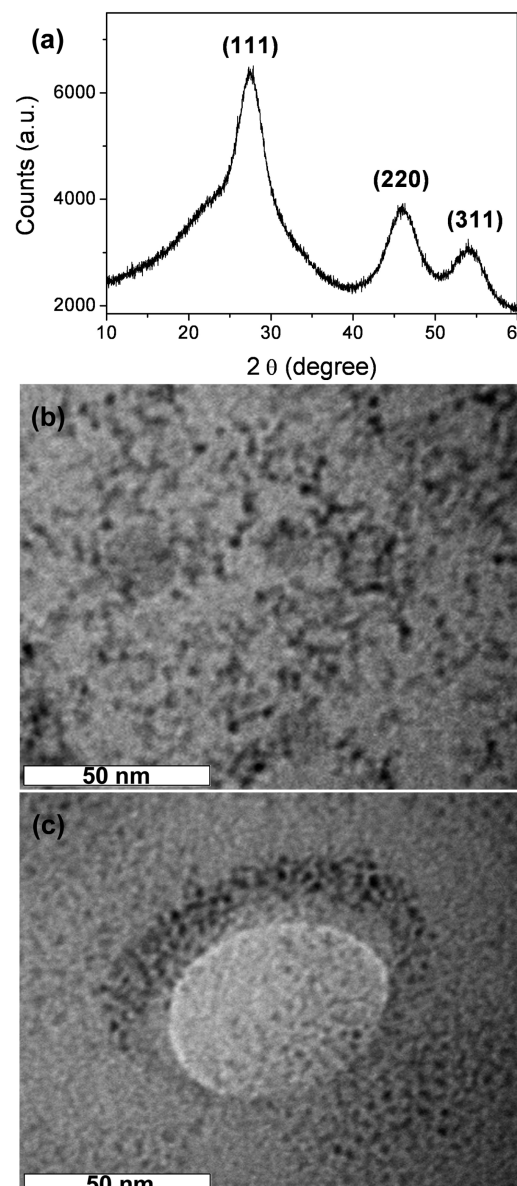


Figure 1. XRD pattern (a) and TEM image (b) of ZnSe:Cu NCs, and TEM image of ZnSe:Mn NCs (c). The Cu/Zn (or Mn/Zn) feed ratio was 0.005/1.

Mn NCs with 8 h reflux. The resultant NCs possessed a cubic zinc blende structure of bulk ZnSe crystal (part a of Figure 1), which was consistent with the previous report.²⁹ Although slight aggregation of NCs was observed under TEM, most NCs appeared as isolated quasi-spherical particles (parts b and c of Figure 1 and Figure S1 of the Supporting Information). Moreover, the presence of Cu or Mn element in doped ZnSe NCs was confirmed by XPS measurement, represented by the appearance of the characteristic Cu 2p_{3/2} peak at 932.1 eV and the Mn 2p_{3/2} peak at 641.4 eV (part c of Figure 2 and Figure S2 of the Supporting Information).

Figure 3 indicated the typical UV-vis absorption spectra and PL spectra of aqueous ZnSe, ZnSe:Cu, and ZnSe:Mn NCs respectively with 0, 1, 4, and 8 h reflux. For ZnSe NCs, an obvious redshift of the 1s–1s excitonic absorption peak was observed during reflux (part a of Figure 3), indicating the size increase of NCs. Moreover, there were two PL emission peaks of the PL spectra of ZnSe NCs (part b of Figure 3). The peak around 390 nm was assigned to the bandgap emission of nanometer-sized ZnSe crystals, and the emission peak over 450

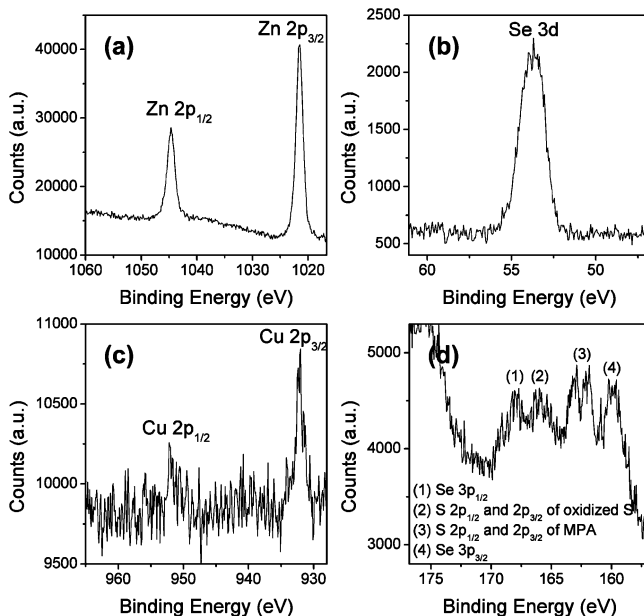


Figure 2. XPS of ZnSe:Cu NCs. The Cu/Zn feed ratio was 0.02/1. (a) Zn 2p spectrum, (b) Se 3d spectrum, (c) Cu 2p spectrum, and (d) S 2p and Se 3p spectra. The presence of the characteristic Zn $2p_{3/2}$ peak at 1021.7 eV, Se 3d peak at 53.9 eV, Cu $2p_{3/2}$ peak at 932.1 eV, and S 2p peaks at 162.0, 163.0, and 166.0 eV indicated the presence of Zn, Se, Cu, and S element in the resulting NCs.

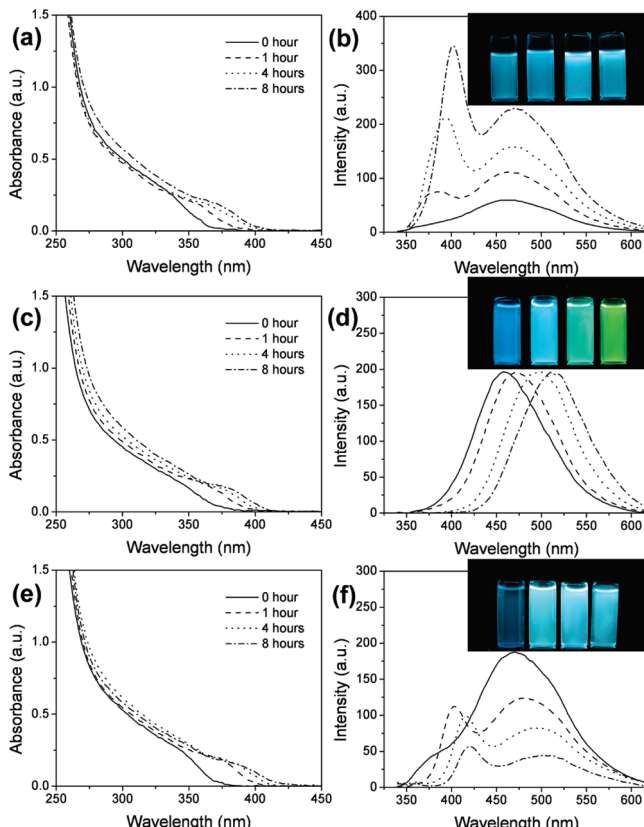


Figure 3. Evolution of the UV-vis absorption spectra (a, c, e) and PL spectra (b, d, f) of ZnSe (a, b), ZnSe:Cu (c, d), and ZnSe:Mn (e, f) NCs during reflux of the precursor solutions at 100 °C for 0 h (solid), 1 h (dash), 4 h (dot), and 8 h (dash dot). The concentration of precursors was 0.01 M, referring to $Zn(NO_3)_2$, whereas the molar ratio of Zn/Cu(Mn)/MPA/Se was fixed at 1:0.005:2.0:0.2. The pH of precursor solutions was 11.5. Inset: fluorescence photographs of NC solutions with 0, 1, 4, and 8 h reflux (from left to right).

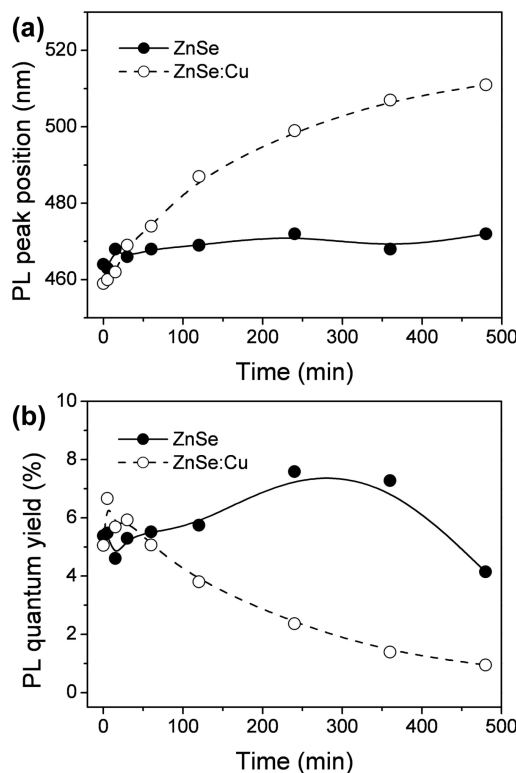


Figure 4. Evolution of PL emission peak positions (a) and PLQYs (b) of ZnSe (solid circle) and ZnSe:Cu (open circle) NCs during reflux of the precursor solutions at 100 °C. The concentration of precursors was 0.01 M, referring to $Zn(NO_3)_2$, whereas the molar ratio of Zn/MPA/Se was fixed at 1:2.0:0.2. For Cu-doped ZnSe, the feed ratio of Cu/Zn was 0.005/1. The pH of precursor solutions was 11.5.

nm was attributed to the trap emission (Figure S3 of the Supporting Information).³² Within 8 hours reflux, a clear redshift of about 20 nm was observed for the bandgap emission, whereas almost no shift was observed for the trap emission (part b of Figure 3). Consequently, the apparent PL was kept blue (inset of part b of Figure 3). This result indicated that the trap emission was less dependent on NC size than the bandgap emission.

In comparison to ZnSe NCs, although the evolution of the absorption spectra of ZnSe:Cu NCs had no obvious difference, the PL spectra were quite different (parts c and d of Figure 3). No bandgap emission was observed for ZnSe:Cu NCs, whereas only the trap emission was exhibited. This result revealed that the doping of a small quality of Cu significantly increased the trap. Meanwhile, the trap emission shifted from 450 to 510 nm with prolonging the reflux duration (part d of Figure 3 and part a of 4), making the apparent PL change from blue to green (part d of Figure 3). Because the trap emission was less dependent on the NC size (part b of Figure 3), the redshift of the PL spectra should be attributed to the Cu dopant; namely, the prolonged reflux facilitated the doping of Cu, which in turn led to the redshift of the trap emission. It should be mentioned that the doping of Cu into bulk ZnSe NCs involved two steps – surface adsorption and internal doping (Figure S4 of the Supporting Information).³² Only the latter contributed to the trap emission. In this context, Cu element first adsorbed on the surface of ZnSe NCs, and was followed by the growth of NCs and/or the surface reaction to incorporate into NCs. Also, note that there was no free Zn^{2+} or Cu^{2+} in NC solution. They were in the form of Zn– or Cu–MPA complexes.⁵² The growth of aqueous NCs was through the adsorption and coalescence of these complexes with host NCs.⁵⁹ ICP measurement revealed that the molar ratio

TABLE 1: Cu/Zn and Mn/Zn Molar Ratio in NCs versus the Reflux Duration of ZnSe:Cu and ZnSe:Mn NCs, Which Was Determined by ICP Measurement^a

reflux duration/minutes	Cu/Zn molar ratio in ZnSe:Cu NCs	Mn/Zn molar ratio in ZnSe:Mn NCs
0	0.0129	0.0039
5	0.0139	0.0172
15	0.0129	0.0130
30	0.0114	0.0110
60	0.0125	0.0113
120	0.0101	0.0117
240	0.0077	0.0094
360	0.0073	0.0095
480	0.0073	0.0081

^a The molar ratio of Zn:MPA:Se was fixed at 1:2.0:0.2, and the Cu/Zn (or Mn/Zn) feed ratio was 0.005/1. The concentration of precursors was 0.01 M, referring to Zn(NO₃)₂. The pH of the precursor solutions was 11.5. As calculated from ICP data, the final doping level was 5.8 Cu atoms per ZnSe:Cu NC (internal doping) and 7.5 Mn atoms per ZnSe:Mn NC (surface doping), respectively.

of Cu/Zn of ZnSe:Cu NCs increased at the first 5 min of reflux (Table 1), indicating that the surface adsorption of Cu–MPA complexes was more favored than those of Zn–MPA complexes. However, the feed ratio of Cu/Zn was only 0.005/1. Prolonged reflux would finally promote the growth of NCs through the coalescence of Zn–MPA complexes with NCs, which also turn the surface adsorption of Cu to internal doping.³² Consequently, although the Cu/Zn ratio of ZnSe:Cu NCs decreased with the long time reflux (Table 1), the internal doping of Cu was favored. Furthermore, the chemical stability of the colloidal solution of ZnSe:Cu NCs was worse than that of ZnSe NCs. Within days of storage, precipitates were observed for ZnSe:Cu NCs, whereas ZnSe NCs could be stored for weeks without precipitation. Note that the precipitates resulted from the oxidation of MPA and NCs, which has been studied by Peng et al. (Figure S5 of the Supporting Information).⁶² Because of this poor stability, moreover, the PLQYs of ZnSe:Cu NCs were generally lower than ZnSe NCs (part b of Figure 4). Detailed discussions were presented in the following sections.

In comparison to ZnSe and ZnSe:Cu NCs, although the same feed ratio of Mn/Zn was adopted in the preparation of ZnSe:Mn NCs (0.005/1), and their PL property was in between those of ZnSe and ZnSe:Cu NCs; namely, a less obvious bandgap emission but a clearer shift of trap emission than ZnSe NCs (parts b, d, and f of Figure 3). This result indicated that Mn was doped into ZnSe NCs but the efficiency was worse than Cu.⁴⁵ ICP measurement revealed that the Mn/Zn ratio of ZnSe:Mn NCs was almost the same as that of ZnSe:Cu NCs (Table 1). It meant that although the adsorption ability of Mn–MPA complexes with NCs had less difference in comparison to Cu–MPA complexes, the coalescence ability was worse, making it more difficult to achieve internal doping.³² Moreover, the temporal evolution of the UV–vis absorption spectra and the bandgap emission of PL spectra of ZnSe:Mn NCs exhibited a more obvious redshift than ZnSe:Cu NCs (parts e and f of Figure 3), representing the more rapid growth of ZnSe:Mn NCs. As indicated in Table 2, the zeta potentials of ZnSe:Mn NCs were usually lower than those of ZnSe:Cu NCs, which indicated that the interparticle electrostatic repulsion of ZnSe:Mn NCs was weaker than that of ZnSe:Cu NCs.⁶¹ According to the colloidal stability theory, weaker electrostatic repulsion benefited the growth of aqueous NCs.⁶¹ Furthermore, the chemical stability of the colloidal solution of ZnSe:Mn NCs was better than that

TABLE 2: Temporal Evolution of the Zeta Potential ζ of MPA-Stabilized ZnSe:Cu and ZnSe:Mn NCs^a

reflux duration/minutes	zeta potential/mV	
	ZnSe:Cu	ZnSe:Mn
0	-29.1	-28.8
5	-31.9	-24.1
15	-31.5	-25.9
30	-34.3	-29.8
60	-31.8	-29.0
120	-34.1	-31.6
240	-33.6	-33.1

^a Corresponding UV–vis absorption spectra and PL spectra were indicated in Figure 3.

of ZnSe:Cu NCs. It might be attributed to the difference in the oxidation ability of Cu(II) and Mn(II) in a MPA-stabilized ZnSe system because the stability of aqueous NCs was mainly determined by the oxidation of mercapto-ligands and NCs.

All of these results indicated that the presence of transition-metal-impurities and also the species of the impurities significantly influenced the size and PL evolution and the stability of aqueous ZnSe NCs. In the following sections, the aforementioned influence would be discussed by combining both the redox reaction between metal impurities and MPA and the electrostatic factors of aqueous NCs.

Redox Reaction of Transition-Metal Impurity-Doped ZnSe NCs. As shown in part d of Figure 3, the PL evolution of ZnSe:Cu NCs was promoted by prolonging the reflux duration of NC solution, which was thought to facilitate the internal doping of Cu. However, the stability of ZnSe:Cu NCs was worse than those of pure ZnSe NCs, especially for the samples with a Cu/Zn feed ratio higher than 0.005/1, making it difficult to accurately monitor the influence of Cu on the PL evolution. Consequently, the effect of Cu/Zn feed ratio on the PL evolution was systematically studied by storing the precursors at room temperature (Figure 5) because it was a moderate condition to maintain the evolution of aqueous NCs.⁶⁵

In general, the PL evolution of ZnSe:Cu NCs was facilitated with the increase of Cu/Zn feed ratio (parts a, c, e, and g of Figure 5) because a high Cu/Zn feed ratio in turn increased the amount of adsorbed Cu and hence the internal doped Cu (Table 3). The increase of internal Cu weakened the bandgap emission of ZnSe NCs but enhanced their trap emission, thus facilitating the PL evolution. Besides, similar to ZnSe:Cu NCs with reflux treatment, the stability of NCs with storage treatment also decreased with the increase of the Cu/Zn feed ratio. NCs would precipitate within days of storage at room temperature for the samples with Cu/Zn ratio higher than 0.01/1. This result was attributed to the oxidation of NCs and/or MPA in a ZnSe:Cu–MPA system (Figure S5 of the Supporting Information).⁶² As shown in part c of Figure 2, the XPS characteristic Cu 2p_{3/2} and Cu 2p_{1/2} peaks were centered at 932.1 and 952.0 eV, respectively, indicating the doped Cu was in the form of Cu(I).⁶³ It implied that a redox reaction might occur because the initial form of Cu was Cu(II). The standard reduction potential of E⁰_{Zn²⁺/Zn} was -0.763 V, whereas that of E⁰_{Cu²⁺/Cu⁺} was 0.153 V. It meant Cu(II) was more easily reduced than Zn(II) in a redox system, and generated Cu(I) (Figure S6 of the Supporting Information). The resulting Cu(I) was doped into ZnSe NCs, which facilitated the PL evolution. Note that there was no free Zn²⁺ in NC solution. Zn(II) was in the form of ZnSe or Zn–MPA complexes with a different Zn/MPA ratio, such as Zn(MPA), Zn(MPA)₂²⁻, and Zn(MPA)₃⁴⁻ (Scheme 1).⁵² Similarly, Cu(II)

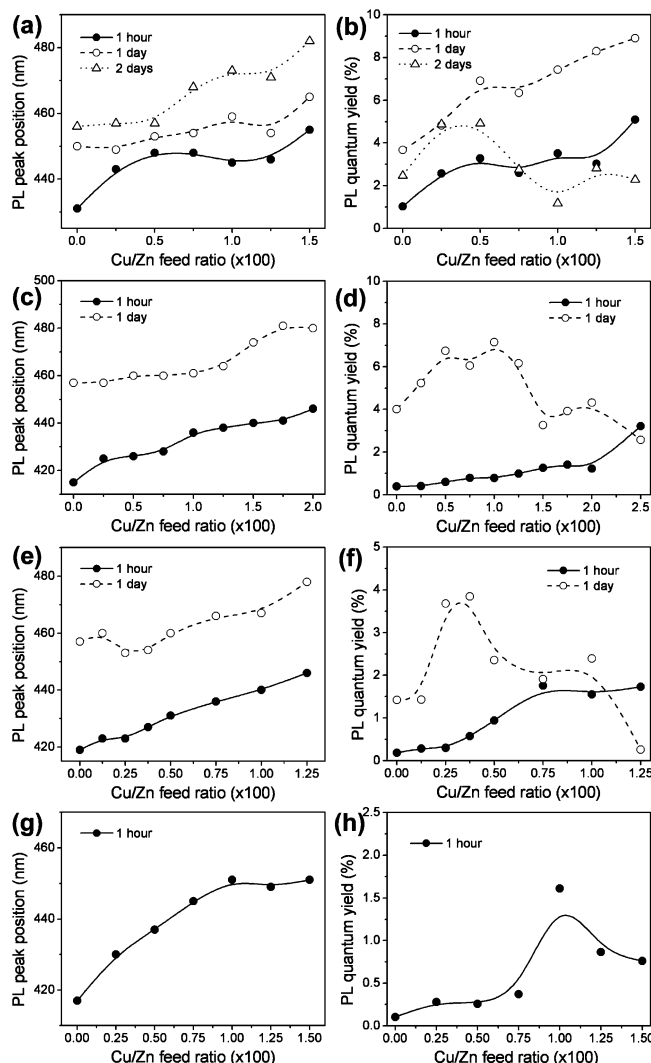


Figure 5. PL emission peak positions (a, c, e, g) and PLQYs (b, d, f, h) of ZnSe:Cu NCs versus the content of Cu during storage at room temperature for 1 hour (solid circle), 1 day (open circle), and 2 days (open triangle). The molar ratio of Zn/MPA/Se was fixed at 1:2.0:0.2, whereas the concentration of precursors was 0.02 M (a, b), 0.01 M (c, d), 0.005 M (e, f), and 0.002 M (g, h), respectively, referring to $\text{Zn}(\text{NO}_3)_2$. The pH of precursor solutions was 11.5.

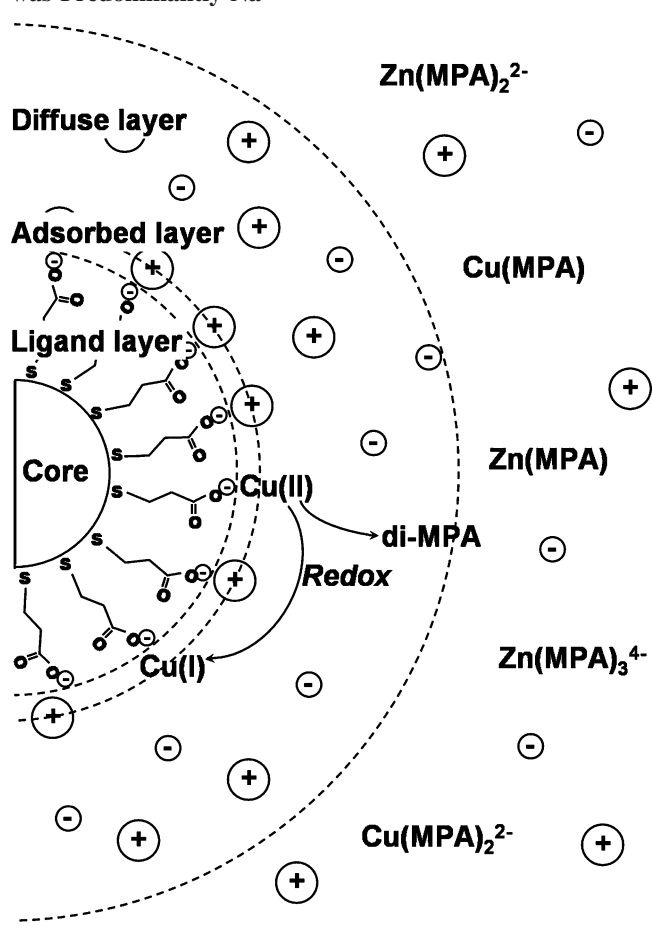
TABLE 3: Cu/Zn Molar Ratio in NCs versus Cu/Zn Feed Ratio, Which Was Determined by ICP Measurement^a

Cu/Zn feed ratio	Cu/Zn molar ratio in NCs
0	0
0.0025	0.0062
0.005	0.0116
0.0075	0.0151
0.01	0.0181
0.0125	0.0217
0.015	0.0216

^a The molar ratio of Zn/MPA/Se was fixed at 1:2.0:0.2, and the concentration of precursors was 0.02 M, referring to $\text{Zn}(\text{NO}_3)_2$. The pH of precursor solutions was 11.5. The preformed precursors were stored for one hour before ICP measurement.

was also in the form of Cu–MPA complexes. Moreover, the –SH group of MPA was a reducing agent, which protected aqueous NCs against oxidation by generating disulfides of MPA (di-MPA).⁶² Namely, instead of the oxidation of ZnSe NCs, MPA first oxidized on the NC surface, whereas NC acted as a catalytic center and Cu(II) acted as an oxidant. In

SCHEME 1: Schematic Illustration of the Electric Double-Layer and Redox Reaction of Aqueous ZnSe:Cu NCs that Were Stabilized by MPA; The Adsorbed Cation was Predominantly Na^+



our experiment, two groups of S 2p_{1/2} and S 2p_{3/2} peaks were observed for the XPS of the S 2p spectrum (part d of Figure 2). It indicated that besides the –SH group of MPA, oxidized S also existed. Furthermore, the di-MPA could be replaced by the excess MPA in the solution. Thus, NCs would not oxidize until the excess MPA was used up.⁶² Consequently, the redox reaction of the ZnSe:Cu–MPA system should occur on the NC surface and between MPA and Cu(II), whereas the final products were Cu(I) and the di-MPA (Scheme 1). The increase of the Cu/Zn feed ratio increased the amount of oxidant and promoted the oxidation of MPA, thus decreasing the stability of NCs.

Moreover, the chemical stability of ZnSe:Cu NCs decreased with lowering NC concentration. The 0.02 M NCs could be stored for three days without any precipitates whatever the Cu/Zn ratio. Within 1 day's storage, however, serious precipitation was observed for 0.002 M NCs with a high Cu/Zn feed ratio. NCs of 0.01 and 0.005 M could be stored for 2 days without precipitates. Consequently, Figure 5 only presented the PL evolution of stable NCs. Note that the concentration-dependent stability of ZnSe:Cu NCs was also attributed to the redox reaction between Cu(II) and MPA. For NC solutions with high concentrations, there was more excess MPA in solution. The excess MPA efficiently prevented the oxidation of NCs, thus increasing the stability (Figure S5 of the Supporting Information).⁶²

The evolution of PLQYs also related to the redox reaction between Cu(II) and MPA, which involved the Cu/Zn feed ratio,

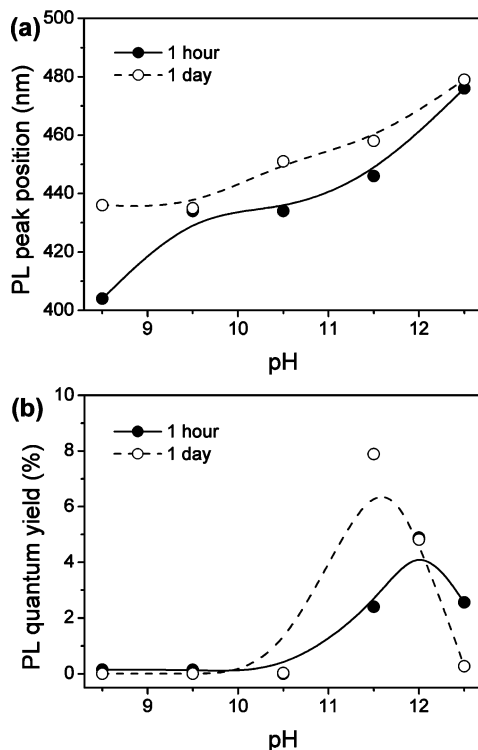


Figure 6. PL emission peak positions (a) and PLQYs (b) of ZnSe:Cu NCs versus pH values during storage at room temperature for 1 hour (solid circle) and 1 day (open circle). The concentration of precursors was 0.01 M, referring to $\text{Zn}(\text{NO}_3)_2$, and the molar ratio of $\text{Zn}/\text{Cu}/\text{MPA}/\text{Se}$ was fixed at 1:0.005:2.0:0.2.

NC concentration, and the duration of storage. In general, the PLQYs increased with the increase of the Cu/Zn feed ratio at proper NC concentration and storage duration, indicating that the Cu dopant actually promoted the trap emission and therefore the corresponding PLQYs (parts b, d, f, and h of Figure 5). Note that the incorporation of Cu into ZnSe NCs was through the redox reaction between Cu(II) and MPA. The increase of the Cu/Zn feed ratio promoted this process. Besides, for the NCs with a specific Cu/Zn feed ratio, the PLQYs also depended on the concentration of NCs and the duration of storage. Except 0.002 M NCs, the QYs increased during 1 day of storage and achieved a maximum. This PL enhancement was attributed to the optimization of the MPA layer on the NC surface during storage (Scheme 1), which efficiently decreased the surface defect and increased the QYs.⁶⁵ Furthermore, the QYs would finally decrease with prolonged storage. A clear decrease of QYs was usually observed before NC precipitation. It was attributed to the oxidation of MPA and the abscission of di-MPA from NCs. The partial absence of the protecting MPA layer increased the surface defects and therefore the decrease of QYs.⁶² The oxidation of MPA was facilitated by increasing the Cu/Zn feed ratio. For example, although the QY of 0.02 M NCs with 1 day of storage and a 0.015:1 Cu/Zn ratio was 9%, and the QY dramatically decreased to 2% after 2 days of storage (part b of Figure 5). Instead, the QYs had no change for the NCs with a 0.0025:1 Cu/Zn ratio. The aforementioned results demonstrated that the evolution of PLQYs of ZnSe NCs was promoted by the Cu(I) dopant, both for the PL enhancement at the initial storage and the PL decrease before precipitation.

It should be mentioned that the evolution of QYs of ZnSe:Cu NCs became more rapid with decreasing NC concentration. Especially, for 0.002 M NCs, a clear decrease of QYs was observed within 1 hour of storage when the Cu/Zn feed ratio

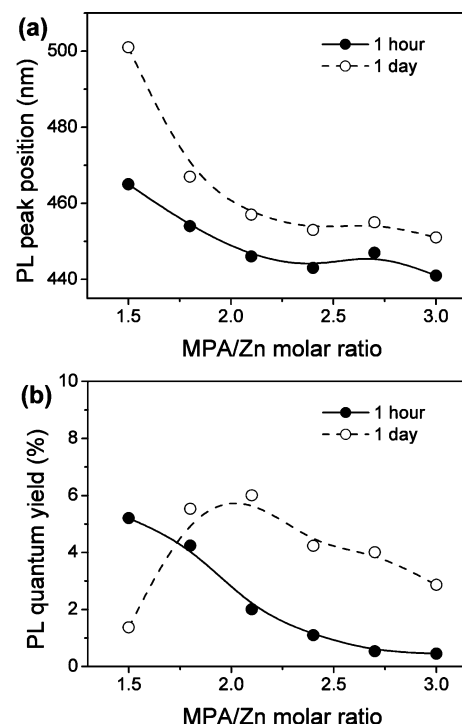


Figure 7. PL emission peak positions (a) and PLQYs (b) of ZnSe:Cu NCs versus MPA to Zn molar ratio during storage at room temperature for one hour (solid circle) and one day (open circle). The concentration of precursors was 0.01 M, referring to $\text{Zn}(\text{NO}_3)_2$, whereas the molar ratio of $\text{Zn}/\text{Cu}/\text{Se}$ was fixed at 1:0.005:0.2. The pH of precursor solutions was 11.5.

was higher than 0.01 (part h of Figure 5). This result firmly proved that the evolution of QYs was essentially determined by the redox reaction between Cu(II) and MPA. In this case, for 0.002 M NCs, the concentration of excess MPA in NC solution was low (0.0048 M), which was rapidly consumed by Cu(II). Thus, there was not enough MPA to protect NCs against oxidation and therefore the poor stability and the rapid decrease of PLQYs.

Furthermore, the standard reduction potential of $E_{\text{Mn}^{2+}/\text{Mn}}^0$ was -1.185 V , which was smaller than both $E_{\text{Zn}^{2+}/\text{Zn}}^0$ and $E_{\text{Cu}^{2+}/\text{Cu}^+}^0$. This meant that, in the ZnSe:Mn system, Mn(II) was difficult to be reduced and doped into ZnSe NCs. In our experiment, a less obvious redshift of the trap emission of ZnSe:Mn NCs was observed in comparison to ZnSe:Cu NCs, which was consistent with the theoretical estimation (parts d and f of Figure 3).

Electrostatics of ZnSe:Cu NCs. Note that the redox reaction between Cu(II) and MPA, in addition to the doping of Cu(I), occurred on NC surfaces, implying that the capability of adsorption of Cu(II) on NCs should influence this process. The experimental variables that facilitated the adsorption of Cu(II) would in turn promote the redox reaction and therefore the Cu(I) doping. Moreover, aqueous NCs were charge-stabilized particles.⁶⁰ The structure and size evolution of them was essentially through the adsorption and coalescence of various ions and clusters.⁵⁹ Consequently, the interparticle electrostatic repulsion was the dominant factor for NC evolution. The experimental variable-dependent PL evolution of ZnSe:Cu NCs should be also comprehended according to the electrostatics of aqueous NCs.

As shown in part a of Figure 6, the PL evolution of ZnSe:Cu NCs was promoted by increasing the pH values of the solution. According to our previous investigations, because of the addition of NaOH for adjusting the pH of NC solution, the increase of

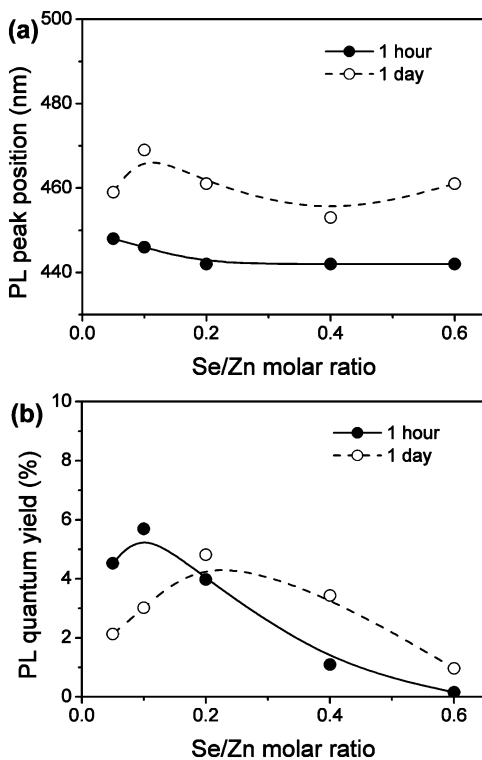


Figure 8. PL emission peak positions (a) and PLQYs (b) of ZnSe:Cu NCs versus Se to Zn molar ratio during storage at room temperature for 1 hour (solid circle) and 1 day (open circle). The concentration of precursors was 0.01 M, referring to $Zn(NO_3)_2$, whereas the molar ratio of $Zn/Cu/MPA$ was fixed at 1:0.005:2.0. The pH of precursor solutions was 11.5.

pH also increased the ionic strength, which weakened the interparticle electrostatic repulsion.⁶¹ It facilitated the adsorption of Cu–MPA complexes on NCs, thus promoting the redox reaction between Cu(II) and MPA and therefore the internal doping of Cu(I). As a result, the PL evolution became faster at high pH values. Similarly, higher QYs were obtained at high pH values (part b of Figure 6) because the generation of a trap emission mainly resulted from the Cu(I) dopant, which was facilitated by the Cu(II) adsorption. However, the QY maximum appeared at pH 12.0 for the NCs with 1 hour of storage, and pH 11.5 for those with 1 day of storage. A further increase of pH led to the decrease of QYs (part b of Figure 6). This was attributed to the poor charge selectivity of the NC diffuse layer to various Zn–MPA complexes at dramatically high pH values, which resulted in the disordered array of Zn and MPA on NC surface.⁶¹ It therefore increased the surface defect and lowered QYs. Moreover, the stability of ZnSe:Cu NCs also decreased with the increase of pH. This result firmly proved the aforementioned consideration that the adsorption and redox reactions of Cu(II) were facilitated at higher pH values, which promoted the evolution of PL and PLQYs.

The PL evolution was also promoted by decreasing the MPA/Zn ratio (Figure 7). Actually, the variation of the MPA/Zn ratio altered the nature of Zn–MPA and Cu–MPA complexes.^{52,61} In this context, the Zn–MPA complexes were in a different form, such as $Zn(MPA)$, $Zn(MPA)_2^{2-}$, and $Zn(MPA)_3^{4-}$.⁵² It was the same for Cu–MPA complexes. The decrease of the MPA/Zn ratio increased the concentration of $Zn(MPA)$ and $Cu(MPA)$ but reduced the average charges of these complexes.⁶¹ Consequently, it became easier for the adsorption and coalescence of complexes on NCs because the move of complexes from solution to the NC surface should traverse through the

diffuse layer of NCs. This diffuse layer generated the electrostatic repulsion between NCs and complexes, whereas the electrostatic repulsion became weaker for the complexes with lower average charges.⁶¹ As a result, the adsorption of Cu(II) on NCs was facilitated at low MPA/Zn ratio, thus benefiting the redox reaction between Cu(II) and MPA. The resulting Cu(I) was doped into ZnSe NCs and facilitated the PL evolution (part a of Figure 7). Moreover, although the initial QY of NCs with a low MPA/Zn ratio, such as 1.5:1, was higher than those with a high MPA/Zn ratio, it decreased during storage (part b of Figure 7). This was attributed to the Cu(II)-generated rapid oxidation of MPA, which was consistent with the previous results (Figure 5 and 6, and Table 3).

Besides, at a lower Se/Zn ratio, ZnSe:Cu NCs also presented more rapid evolution of PL and PLQYs (Figure 8). On the basis of the aforementioned discussions, this result was also comprehensible according to the electrostatics of aqueous NCs. In this context, a low Se/Zn ratio led to excess Zn–MPA and Cu–MPA complexes in the solution and therefore a high ionic strength.⁶¹ It benefited the adsorption of Cu(II) on NCs. Moreover, the decrease of the Se/Zn ratio also increased the concentration of $Zn(MPA)$ and $Cu(MPA)$ but decreased the average charges of these complexes.⁶¹ It also benefited the adsorption of Cu(II) on NCs, which was similar to the decrease of the MPA/Zn ratio. Consequently, the redox reaction between Cu(II) and MPA and Cu(I) doping was facilitated. It led to the rapid evolution of PL and PLQYs.

Conclusions

On the basis of the redox reaction and electrostatics of aqueous NCs, the influence of bivalent transition-metal impurities on the PL evolution of ZnSe NCs was systematically analyzed. The doping process involved the adsorption of metal impurities and the reduction of them by MPA on NC surfaces, which was comprehensible according to two aspects. First, the PL emission of doped NCs was a trap emission. The introduction of metal impurities benefited the trap emission, thus promoting the PL evolution. However, the increase of impurities also promoted the oxidation of MPA, leading to a dramatic decrease of NC stability. Second, aqueous NCs were essentially stabilized by their surface charges through the interparticle electrostatic repulsion. The structure and size evolution of metal impurity-doped ZnSe NCs were through the adsorption and coalescence of various ions and clusters on NC surfaces. Consequently, the electrostatic factors that benefited the adsorption of metal impurities would facilitate the redox reaction, represented by the pH effect and the effects of MPA/Zn and Se/Zn ratio. On the basis of these investigations, the experimental variable-dependent PL evolution and stability of transition-metal impurity-doped aqueous NCs became understandable.

Acknowledgment. This work was supported by NSFC (20704014, 20534040, 20731160002), the 973 Program of China (2007CB936402, 2009CB939701), the FANEDD of China (200734), and the Program for New Century Excellent Talents in University.

Supporting Information Available: Low-magnification TEM image of ZnSe:Cu NCs, XPS Mn 2p spectrum of ZnSe:Mn NCs, schematic illustrations of the levels of doped ZnSe NCs, surface adsorption and internal doping of copper, mechanism of the aggregation of ZnSe:Cu NCs, and the comparison of $E_{Zn^{2+}/Zn}$ and E_{Cu^{2+}/Cu^+} in ZnSe:Cu–MPA system. This material is available free of charge via the Internet at <http://pubs.acs.org>.

References and Notes

- (1) Murray, C. B.; Norris, D. J.; Bawendi, M. G. *J. Am. Chem. Soc.* **1993**, *115*, 8706.
- (2) Wang, X.; Zhuang, J.; Peng, Q.; Li, Y. *Nature (London)* **2005**, *437*, 121.
- (3) Milliron, D. J.; Hughes, S. M.; Cui, Y.; Manna, L.; Li, J.; Wang, L.; Alivisatos, A. P. *Nature (London)* **2004**, *430*, 190.
- (4) Yin, Y.; Alivisatos, A. P. *Nature (London)* **2005**, *437*, 664.
- (5) Tang, Z.; Kotov, N. A.; Giersig, M. *Science* **2002**, *297*, 237.
- (6) Klimov, V. I.; Mikhailovsky, A. A.; Xu, S.; Malko, A.; Hollingsworth, J. A.; Leatherdale, C. A.; Eisler, H. J.; Bawendi, M. G. *Science* **2000**, *290*, 314.
- (7) Chan, W. C. W.; Nie, S. *Science* **1998**, *281*, 2016.
- (8) Agrawal, M.; Rubio-Retama, J.; Zafeiropoulos, N. E.; Gaponik, N.; Gupta, S.; Cimrova, V.; Lesnyak, V.; López-Cabarcos, E.; Tzavalas, S.; Rojas-Reyna, R.; Eychmüller, A.; Stamm, M. *Langmuir* **2008**, *24*, 9820.
- (9) Wang, L.; Wang, X.; Xu, M. F.; Chen, D. D.; Sun, J. Q. *Langmuir* **2008**, *24*, 1902.
- (10) Yu, W. W.; Peng, X. G. *Angew. Chem., Int. Ed.* **2002**, *41*, 2368.
- (11) Peng, Z. A.; Peng, X. G. *J. Am. Chem. Soc.* **2001**, *123*, 183.
- (12) Murphy, C. J. *J. Mater. Chem.* **2008**, *18*, 2173.
- (13) Dai, Q. Q.; Xiao, N. R.; Ning, J. J.; Li, C. Y.; Li, D. M.; Zou, B.; Yu, W. W.; Kan, S. H.; Chen, H. Y.; Liu, B. B.; Zou, G. T. *J. Phys. Chem. C* **2008**, *112*, 7567.
- (14) Qu, L.; Peng, Z. A.; Peng, X. G. *Nano Lett.* **2001**, *1*, 333.
- (15) Xie, R. G.; Peng, X. G. *Angew. Chem., Int. Ed.* **2008**, *47*, 7677.
- (16) Rajh, T.; Mićić, O. I.; Nozik, A. J. *J. Phys. Chem.* **1993**, *97*, 11999.
- (17) Rogach, A. L.; Franzl, T.; Klar, T. A.; Feldmann, J.; Gaponik, N.; Lesnyak, V.; Shavel, A.; Eychmüller, A.; Rakovich, Y. P.; Donegan, J. F. *J. Phys. Chem. C* **2007**, *111*, 14628.
- (18) Gao, M.; Kirstein, S.; Möhwald, H.; Rogach, A. L.; Kornowski, A.; Eychmüller, A.; Weller, H. *J. Phys. Chem. B* **1998**, *102*, 8360.
- (19) Zhang, H.; Zhou, Z.; Yang, B.; Gao, M. Y. *J. Phys. Chem. B* **2003**, *107*, 8.
- (20) Zhang, H.; Wang, L.; Xiong, H.; Hu, L.; Yang, B.; Li, W. *Adv. Mater.* **2003**, *15*, 1712.
- (21) Li, L.; Qian, H.; Ren, J. *Chem. Commun.* **2005**, 528.
- (22) Bao, H. F.; Wang, E. K.; Dong, S. J. *Small* **2006**, *2*, 476.
- (23) He, Y.; Sai, L. M.; Lu, H. T.; Hu, M.; Lai, W. Y.; Fan, Q. L.; Wang, L. H.; Huang, W. *Chem. Mater.* **2007**, *19*, 359.
- (24) Wang, C. L.; Zhang, H.; Zhang, J. H.; Li, M. J.; Sun, H. Z.; Yang, B. *J. Phys. Chem. C* **2007**, *111*, 2465.
- (25) Liu, Y.; Shen, Q. H.; Yu, D. D.; Shi, W. G.; Li, J. X.; Zhou, J. G.; Liu, X. Y. *Nanotechnology* **2008**, *19*, 245601.
- (26) Gu, Z. Y.; Zou, L.; Fang, Z.; Zhu, W. H.; Zhong, X. H. *Nanotechnology* **2008**, *19*, 135604.
- (27) Bang, J. H.; Suh, W. H.; Suslick, K. S. *Chem. Mater.* **2008**, *20*, 4033.
- (28) Qian, H. F.; Dong, C. Q.; Peng, J. L.; Qiu, X.; Xu, Y. H.; Ren, J. C. *J. Phys. Chem. C* **2007**, *111*, 16852.
- (29) Zheng, Y. G.; Yang, Z. C.; Ying, J. Y. *Adv. Mater.* **2007**, *19*, 1475.
- (30) Liu, F. C.; Cheng, T. L.; Shen, C. C.; Tseng, W. L.; Chiang, M. Y. *Langmuir* **2008**, *24*, 2162.
- (31) Pradhan, N.; Peng, X. G. *J. Am. Chem. Soc.* **2007**, *129*, 3339.
- (32) Pradhan, N.; Goorskey, D.; Thessing, J.; Peng, X. G. *J. Am. Chem. Soc.* **2005**, *127*, 17586.
- (33) Lan, G. Y.; Lin, Y. W.; Huang, Y. F.; Chang, H. T. *J. Mater. Chem.* **2007**, *17*, 2661.
- (34) Murase, N.; Gao, M. Y. *Mater. Lett.* **2004**, *58*, 3898.
- (35) Li, C. L.; Nishikawa, K.; Ando, M.; Enomoto, H.; Murase, N. *Colloids Surf. A* **2007**, *294*, 33.
- (36) Qian, H. F.; Qiu, X.; Li, L.; Ren, J. C. *J. Phys. Chem. B* **2006**, *110*, 9034.
- (37) Du, M. H.; Erwin, S. C.; Efros, A. L. *Nano Lett.* **2008**, *8*, 2878.
- (38) Yang, H.; Santra, S.; Holloway, P. H. *J. Nanosci. Nanotech.* **2005**, *5*, 1364.
- (39) Datta, A.; Biswas, S.; Kar, S.; Chaudhuri, S. *J. Nanosci. Nanotechnol.* **2007**, *7*, 3670.
- (40) Nag, A.; Chakraborty, S.; Sarma, D. D. *J. Am. Chem. Soc.* **2008**, *130*, 10605.
- (41) Zhuang, J. Q.; Zhang, X. D.; Wang, G.; Li, D. M.; Yang, W. S.; Li, T. J. *J. Mater. Chem.* **2003**, *13*, 1853.
- (42) Beaulac, R.; Archer, P. I.; Rijssel, J. V.; Meijerink, A.; Gamelin, D. R. *Nano Lett.* **2008**, *8*, 2949.
- (43) Pradhan, N.; Battaglia, D. M.; Liu, Y. C.; Peng, X. G. *Nano Lett.* **2007**, *7*, 312.
- (44) Althues, H.; Palkovits, R.; Rumplecker, A.; Simon, P.; Sigle, W.; Bredol, M.; Kynast, U.; Kaskel, S. *Chem. Mater.* **2006**, *18*, 1068.
- (45) Li, J. B.; Wei, S. H.; Li, S. S.; Xia, J. B. *Phys. Rev. B* **2008**, *77*, 113304.
- (46) Xing, G. C.; Ji, W.; Zheng, Y. G.; Ying, J. Y. *Opt. Express* **2008**, *16*, 5710.
- (47) Chon, J. W. M.; Gu, M.; Bullen, C.; Mulvaney, P. *Appl. Phys. Lett.* **2004**, *84*, 4472.
- (48) Lad, A. D.; Kiran, P. P.; Kumar, G. R.; Mahamuni, S. *Appl. Phys. Lett.* **2007**, *90*, 133113.
- (49) Suyver, J. F.; Beek, T. V. D.; Wuister, S. F.; Kelly, J. J.; Meijerink, A. *Appl. Phys. Lett.* **2001**, *79*, 4222.
- (50) Piepenbrock, M. M.; Stirner, T.; O'Neill, M.; Kelly, S. M. *J. Am. Chem. Soc.* **2007**, *129*, 7674.
- (51) Guo, J.; Yang, W. L.; Wang, C. C. *J. Phys. Chem. B* **2005**, *109*, 17467.
- (52) Shavel, A.; Gaponik, N.; Eychmüller, A. *J. Phys. Chem. B* **2006**, *110*, 19280.
- (53) Zhao, K.; Li, J.; Wang, H. Z.; Zhuang, J. Q.; Yang, W. S. *J. Phys. Chem. C* **2007**, *111*, 5618.
- (54) Mandal, A.; Tamai, N. *J. Phys. Chem. C* **2008**, *112*, 8244.
- (55) Li, C.; Murase, N. *Chem. Lett.* **2005**, *34*, 92.
- (56) Li, J.; Hong, X.; Li, D.; Zhao, K.; Wang, L.; Wang, H.; Du, Z.; Li, J.; Bai, Y.; Li, T. *Chem. Commun.* **2004**, 1740.
- (57) Liu, Y.; Chen, W.; Joly, A. G.; Wang, Y.; Pope, C.; Zhang, Y.; Bovin, J. O.; Sherwood, P. *J. Phys. Chem. B* **2006**, *110*, 16992.
- (58) Schulz-Drost, C.; Sgobba, V.; Guldi, D. M. *J. Phys. Chem. C* **2007**, *111*, 9694.
- (59) Zhang, H.; Wang, D. Y.; Yang, B.; Möhwald, H. *J. Am. Chem. Soc.* **2006**, *128*, 10171.
- (60) Zhang, H.; Liu, Y.; Zhang, J. H.; Wang, C. L.; Li, M. J.; Yang, B. *J. Phys. Chem. C* **2008**, *112*, 1885.
- (61) Zhang, H.; Liu, Y.; Wang, C. L.; Zhang, J. H.; Sun, H. Z.; Li, M. J.; Yang, B. *ChemPhysChem* **2008**, *9*, 1309.
- (62) Aldana, J.; Wang, Y. A.; Peng, X. G. *J. Am. Chem. Soc.* **2001**, *123*, 8844.
- (63) Hao, E. C.; Zhang, H.; Yang, B.; Ren, H.; Shen, J. C. *J. Colloid Interface Sci.* **2001**, *238*, 285.
- (64) Talapin, D. V.; Rogach, A. L.; Shevchenko, E. V.; Kornowski, A.; Haase, M.; Weller, H. *J. Am. Chem. Soc.* **2002**, *124*, 5782.
- (65) Wang, C. L.; Zhang, H.; Zhang, J. H.; Lü, N.; Li, M. J.; Sun, H. Z.; Yang, B. *J. Phys. Chem. C* **2008**, *112*, 6330.

JP810165P